Theory of the Kinetics of the Helix–Coil Transition in Two-Chain, Coiled Coils. 2. The Finite Chain

Jeffrey Skolnick†

Department of Chemistry, Washington University, St. Louis, Missouri 63130.
Received March 16, 1984

ABSTRACT: The kinetic Ising, neglect-loop-entropy, perfect matching model of the helix–coil transition in two-chain, coiled coils applied previously to infinite chains has been extended to include chains of moderate to infinite length. Based on the approximate analytical form for the equilibrium helix probability profiles, a derivation is presented of an approximate master equation for the time dependence of the conformational state of the jth residue, expressed as an occupation number, $q_j(t)$. Analytic solutions for $q_j(t)$ and the mean occupation number, $\bar{q}(t)$, are presented. The approximate solution gives the exact initial slope, λ_0 (i.e., the initial slope obtained from the exact master equation), for the normalized time-dependent helix content, $H(t)$, vs. time. The validity of the method is checked by comparing the approximate infinite-time overall helix content consistent with λ_0 to the exact equilibrium value. Application is made to a homopolymeric analogue of tropomyosin for varying initial and final states, and an examination of the range of validity of the initial slope approximation to $H(t)$ is undertaken. Finally, a comparison of the kinetics of the helix–coil transition in two-chain, coiled coils and analogous single-chain homopolypeptides is made.

I. Introduction

Of late, there has been an increasing interest in the dynamics of protein folding, and various mechanisms have been proposed to describe the kinetics of these processes in globular proteins.[1,2] However, the folding process in globular proteins is extremely complicated, and we therefore believe it is worthwhile to examine the nature of the kinetics of the helix–coil transition in a far simpler system: the α-helical, two-chain, coiled coils. An understanding of the kinetics of the helix–coil transition in two-chain, coiled coils (dimers) not only is interesting in its own right, but may also provide insight into some aspects of the early steps of chain folding in globular proteins.[3] With this objective in mind, in a recent paper, hereinafter designated paper 1,[4] we began the development of the theory of the kinetics of the helix–coil transition in α-helical, two-chain, coiled coils and focused explicitly on the infinite-chain limit. Employing the insight gained from that study, we develop in what follows the theory applicable to finite chains.

In paper 1, we formulated the simplest kinetic Ising model[5] of the two-chain helix–coil transition that contains what we believe are many, but not all, important aspects of the physics. In particular, the following assumptions common to both the equilibrium and kinetic description of the helix–coil transition are invoked. The theory is formulated in terms of the "short-range" Zimm–Bragg helix initiation parameter, σ, and propagation parameter, s, which are assumed to depend only on the type of amino acid and not on the type or conformation of nearest neighbors.[6] "Long-range" interactions between chains are accounted for by an interhelical interaction parameter w^0.[7] Furthermore, interacting helical segments are assumed to remain parallel and in-register throughout the course of the conformational transition; i.e., mismatch is neglected. The effects of loop entropy are ignored. A more detailed discussion of the validity of these assumptions can be found in previous work.[4,7-10]

For chains of all lengths, a more realistic model would recognize that both chains need to be oriented properly to effect the helix–helix interaction. Thus, at equilibrium, the first pair of residues in an interacting helical stretch should have statistical weight $v\sigma^2s^2w$, wherein v takes account of the orientational factor between the two chains. It is a straightforward matter to incorporate v into the equilibrium theory as well as the kinetic Ising, neglect-loop-entropy model. However, at present the value of v is unknown and here we take the simplest case and set $v = 1.0$.

The following additional assumptions are invoked to characterize the kinetics. The transition probability, that is, the probability per unit time that the jth residue jumps from a helix to a random coil state or vice versa, depends on the state of the jth residue and residues $j \pm 1$; hence, Schwarz's kinetic parameters γ_H and γ_C are both set equal to $2/(1 + \sigma)$.[11,12] Furthermore, the equilibrium parameters σ, s, w^0 required in the calculation of the transition probability are those of the infinite-time, equilibrium final state. Finally, we assume that the rate of the helix–coil transition is not diffusion controlled. We would expect this to be quite reasonable for the helix–coil transition (in which the initial state comprises only associated dimers) as is probed in, say, a temperature-jump experiment (the helix content of two-chain, coiled coils such as tropomyosin decreases with increasing temperature[13-15]). We would expect this assumption along with neglect of mismatch to be more questionable in the case of renaturation, that is, for a temperature-drop experiment. With the neglect of mismatch and chain–chain diffusion, we are in essence treating the helix–coil dynamics of two benignly tethered chains. We refer the reader to paper 1 for a deeper discussion of these assumptions.

The foregoing assumptions provide us with a well-defined kinetic Ising model and allow us to follow the method of Glauber[5] in formulating a master equation for the time dependence of the helix content of the jth residue. Let us define the instantaneous occupation number

$\mu_j = +1$ if the jth residue is in a helical state

$= -1$ if the jth residue is in a random coil state

As is typical of many-body problems, there is an infinite hierarchy of coupled equations for the correlation functions (in this case coupled first-order differential equations), in which we need the time dependence of the $(n + 1)$th-order correlation function to determine the time dependence of the nth-order correlation function. In the case of infinite chains, it is possible to close the hierarchy by replacing three-site and higher order correlation functions by lower order correlation functions in the master equations for the time dependence of the mean occupation number and of the site–site correlation functions. This approximation is motivated by the cooperative nature of the transition in

† Alfred P. Sloan Foundation Fellow.

0024-9297/85/2218-0232$01.50/0

that nearest-neighbor residues on the same chain and in different chains will tend to be in the same conformational state and will also tend to flip simultaneously. A very similar closure approximation for the autocorrelation function of the occupation number in single-chain polypeptides and DNA type helices has been employed by Tanaka, Wada, and Suzuki.[16]

For the case of two-chain, coiled coils of infinite length, we found (in paper 1) that virtually the entire relaxation spectrum for both large and relatively small perturbations from the initial state is well characterized by the slowest relaxing mode. Physically, the slowest relaxing mode is a very long wavelength, cooperative mode in which domains of mean length on the order of $1/\sigma^{1/2}$ monomer units flip on the average in the direction of the final equilibrium state. We found the rate constant corresponding to this slowest relaxing mode in dimers to be almost independent of final-state helix content over an appreciable range (for the case calculated in paper 1, helix contents in the range of 8.2–90.5%), and it is well approximated by the rate constant corresponding to a final state of 50% helix content. Thus, it reflects the dominant role played by the cooperativity in the dynamics of the helix–coil transition. Hence, the rate of the helix–coil transition from a high initial helix content to a low final helix content or vice versa may be estimated by probing the kinetics near the transition midpoint. Moreover, for infinite chains, we found that the time scale for relatively large perturbations from the initial state is similar in two-chain, coiled coils and single chains; but because of the more cooperative nature of the transition in dimers, the slowest relaxing mode is a more adequate characterization of the dynamics over a larger range of final states in dimers than in single chains. Finally, we concluded that temperature-jump measurements employing a uniform temperature increment probe the quasi-equilibrium regime at low and high temperatures and probe the relatively large perturbation from equilibrium regime in the vicinity of the transition midpoint.

In this paper, we shall extend the kinetic Ising, neglect-loop-entropy, perfect matching model to chains of finite length. In section II, because of the intimate connection of the master equation to the structure of the equilibrium solution, we begin by constructing an approximate analytic form for the equilibrium helix probability profiles. This approximate analytic form is valid for chains of moderate to infinite length where the slope of the helix probability vs. residue number is not too large. We then derive an approximate master equation for the occupation number consistent with the approximate analytic form of the infinite-time, equilibrium helix content. Moreover, we assume that the site–site correlation functions at time t may be replaced by their infinite-time values, an approximation that is valid if the initial and final states are not too far apart or if the coupling constant reflecting the bias to a helical or random coiled state is not too large. Furthermore, this approximation is consistent with the infinite-chain, $N = \infty$, limit derived previously in paper 1. For chains of finite length, analytic expressions for the time dependence of the mean helix content of the jth residue and for the overall mean helix content are derived, as are expressions for the exact initial slope λ_0. The initial slope is employed to fix the parameter necessary in the calculation of the dynamics as well as the infinite-time, approximate analytic form of the helix content.

In section III, we present numerical results for the time dependence of the overall helix content in a homopolymeric analogue of the prototypical two-chain, coiled-coil tropomyosin, for various initial and final states. Furthermore, a discussion of the validity of the approximate solution introduced in section II is undertaken, and the utility of the initial slope characterization of the dynamics is examined over a wide range of initial and final states. Finally, a comparison with the kinetics in an analogous single-chain homopolypeptide is made. Section IV summarizes the conclusions of the present paper and points out directions of future work.

II. Formulation of the Finite-Chain, Kinetic Ising, Neglect-Loop-Entropy, Perfect Matching Model

A. General Considerations. Consider a homopolymeric, in-register, two-chain, coiled coil, each chain of which consists of $N - 1$ residues, plus two appended phantom, randomly coiled residues attached to the ends. Denote the instantaneous occupation number of the jth residue in chains one and two by μ_j and μ_j^0, respectively. In all that follows a superscript zero labels the second chain. Let us define the expectation value of the occupation number of the jth residue in chain one (two) by $q_j(t)$ ($q_j^0(t)$) wherein the μ_j (μ_j^0) are to be regarded as stochastic functions of time. That is

$$q_j = \langle \mu_j(t) \rangle \tag{II-1}$$

where $\langle\ \rangle$ denotes the ensemble average.

Since by hypothesis the two chains are identical, we need only focus on the correlation functions between residues in chain one and the cross correlation functions between residues in chain one and chain two.

In particular, we shall require the expectation values of site–site correlation functions

$$r_{j,k}(t) = \langle \mu_j(t)\mu_k(t) \rangle \tag{II-2a}$$

$$r_{j,k^0}(t) = \langle \mu_j(t)\mu_k{}^0(t) \rangle \tag{II-2b}$$

In section II of paper 1, we demonstrated that $q_j(t)$ evolves in time according to eq 1-II-12b as (in the following, equations in paper 1 are referred to by a prefix 1; e.g., 1-II-12b is eq II-12b of paper 1)

$$\frac{dq_j}{dt} = -\alpha\Bigg\{(1-\delta)q_j - \frac{\gamma}{2}(q_{j-1} + q_{j+1}) + \frac{\gamma\delta}{2}(\langle \mu_j\mu_j{}^0\mu_{j+1}\rangle + \langle \mu_j\mu_j{}^0\mu_{j-1}\rangle) - \beta + \frac{\beta\gamma}{2}(r_{j-1,j} + r_{j+1,j}) + \beta\delta r_{j,j^0} - \frac{\beta\gamma\delta}{2}(r_{j-1,j^0} + r_{j+1,j^0})\Bigg\} \tag{II-3a}$$

$$dq_j/dt = -\alpha\chi_j(t) \tag{II-3b}$$

in which time dependence of $r_{j,k}(t)$ and $r_{j,k^0}(t)$ is given in eq 1-II-14 and 1-II-15, respectively. In eq II-3a, α sets the fundamental time scale for the process and has the dimensions of time^{-1}; γ plays the role of the *intrachain* cooperativity parameter and is defined by

$$\gamma = \frac{1-\sigma}{1+\sigma} \tag{II-4a}$$

δ is the *interchain* cooperativity parameter

$$\delta = ((w^0)^{1/2} - 1)/((w^0)^{1/2} + 1) \tag{II-4b}$$

and

$$\beta = (s(w^0)^{1/2} - 1)/(s(w^0)^{1/2} + 1) \tag{II-4c}$$

reflects the bias to helical ($\beta > 0$; $s(w^0)^{1/2} > 1$), or random coil ($\beta < 0$; $s(w^0)^{1/2} < 1$) states, i.e., indicates the overall direction of the process. Observe that with finite chains,

the residues in dimer are no longer translationally invariant; hence, even if we make the same level of approximations as in the infinite-chain limit to truncate the infinite hierarchy, we have to solve $(N-1)(3N/2-1)$ coupled linear first-order differential equations ($N-1$ for the q_j; $(N-1)(N-2)/2$ for the $r_{j,k}$, and $(N-1)^2$ for r_{j,k^0}). For small chains, this is perhaps a practical approach, but for chains on the order of 284 residues, it clearly is not. Thus, we shall have to develop an approximation to eq II-3a that is numerically more tractable.

B. Approximate Equilibrium Solution. Setting $dq_j/dt = 0$ in eq II-3a provides us with a relationship between the various one-site, two-site, and three-site correlation functions at infinite time (equilibrium). By analogy to the $s = 1$ single-chain case, let us assume that the equilibrium solution to $q_j(\infty)$ is of the form

$$q_j(\infty) = \frac{-(1+q)\cosh[(N/2-j)\theta]}{\cosh\left(\frac{N\theta}{2}\right)} + q \qquad \text{(II-5)}$$

wherein q is the infinite-chain limit of the equilibrium helix content (which can be obtained via Appendix B, paper 1, eq 1-B-8) and θ is a constant to be determined. The form of eq II-5 is quite plausible. Equation II-5 satisfies the boundary condition that $q_0 = q_N = -1$, gives $q_j \to q$ for residues in the middle of the chain, and is exact when $\delta = 0$ (i.e., $w^0 = 1$) and s equals unity. (See eq 1-II-19. Note that $q = 0$ when $w^0 = 1$ and $s = 1$.) If eq II-5 is valid, then the average value of the occupation number defined by

$$\bar{q} = (N-1)^{-1}\sum_{j=1}^{N-1} q_j(\infty) \qquad \text{(II-6a)}$$

is given by

$$\bar{q} = \frac{-(1+q)\sinh[(N-1)\theta/2]}{(N-1)\cosh\frac{N\theta}{2}\sinh(\theta/2)} + q \qquad \text{(II-6b)}$$

The overall mean helix content of the dimer is related to $\bar{q}$ by

$$f_{hd} = (1+\bar{q})/2 \qquad \text{(II-6c)}$$

Equation II-6b is quite reasonable. In limit that $N-1 \to \infty$, $\bar{q} \to q$ and becomes independent of θ. Moreover since $|q| \leq 1$, $\bar{q} \to q$ from below. Because of the randomizing effect of chain ends, the helix content of an infinite chain is always greater than that of a finite chain for the same values of σ, s, and w^0.

Equation II-6b may be viewed as the defining equation for θ; that is, the mean occupation number at finite N (see Appendix, eq A-6) is determined from the exact equilibrium theory and one then uses eq II-6b to solve for θ. One then checks the agreement of the approximate and exact probability profiles. As demonstrated below, θ also enters in the calculation of the initial slope of the normalized time-dependent mean occupation number (and helix content)

$$H(t) = \frac{\bar{q}(t) - \bar{q}(\infty)}{\bar{q}(0) - \bar{q}(\infty)} \qquad \text{(II-7)}$$

vs. time with $\bar{q}(t)$ the mean occupation number at time t. We shall fit θ to the initial slope and compare values of the mean helix content calculated via eq II-6b with the exact helix content (see eq 9 of ref 7).

Let us now examine the conditions under which eq II-6b is consistent with the exact relation of the q_j at infinite time given in eq II-3a. In the limit of moderate to long chains the terms r_{j,j^0}, $r_{j,j\pm1}$, and $r_{j\pm1,j^0}$ are independent of j; that is, we make *approximation I*

$$C_a = 1 - \frac{\gamma}{2}(r_{j,j-1} + r_{j,j+1}) - \delta r_{j,j^0} + \frac{\gamma\delta}{2}(r_{j-1,j^0} + r_{j+1,j^0}) \qquad \text{(II-8a)}$$

where C_a is a constant independent of j. By way of illustration and to examine the validity of this approximation we have calculated

$$D_j = \frac{\gamma}{2}(r_{j,j-1} + r_{j,j+1}) + \delta r_{j,j^0} - \frac{\gamma\delta}{2}(r_{j-1,j^0} + r_{j+1,j^0}) \qquad \text{(II-8b)}$$

as a function of j for a homopolymeric, two-chain, coiled coil, containing 284 residues per chain with $\sigma = 5 \times 10^{-4}$, $s = 0.94$ (the homopolymeric analogue of tropomyosin[8]), and $w^0 = 1.25$ (helix content of 89.2%). It is in the limit of high helix where the probability profile varies most appreciably as a function of j and where the approximation embodied in eq II-8a is tested most severely. We find that D_j varies by less than 0.2% from the value of 0.9872 for the middle residues $51 \leq j \leq 234$ and less than 3.5% from the value of 0.9872 for $20 \leq j \leq 265$. The value of D_1 (and by symmetry D_{284}) is 0.8898. Hence D_j varies by less than about 10% over the entire range of j and is within 3.5% of D_{142} for 86% of the residues. In other words, as expected, the approximation embodied in eq II-8a breaks down near the ends (which are essentially randomly coiled anyway and thus make a very small contribution to the helix–coil kinetics). Hence, we conclude that approximation I, eq II-8a, is justified.

We now make *approximation IIa*

$$\langle \mu_j \mu_j^0 \mu_{j\pm1} \rangle \simeq (1+\epsilon) q_j \qquad \text{(II-9a)}$$

with ϵ a constant independent of j but which may depend on N. Because of the cooperative nature of the transition, $\mu_j \simeq \mu_{j\pm1}$, the factor ϵ corrects for slight deviations due to end effects and compensates for the fact that $\sigma \neq 0$.

We have calculated the ratio

$$S_{j,j\pm1} = \langle \mu_j \mu_j^0 \mu_{j\pm1} \rangle / q_j \qquad \text{(II-9b)}$$

as a function of j. As discussed in the Appendix, $S_{j,j+1} = S_{N-j,N-j-1}$; therefore, we need only examine the behavior of $S_{j,j+1}$ as a function of j. We have calculated $S_{j,j+1}$ vs. j for the same homopolymeric, two-chain, coiled coil discussed above. $S_{j,j+1}$ is within 1.3% of the valued of $S_{142,143}$ of 0.9890 for $20 \leq j \leq 264$. Furthermore, the $N = \infty$ value is 0.9890. The worst disagreement is at $j = 10$ where $S_{10,11} = 1.250$ (this is where $q_j \to 0$). Thus, except near the ends eq II-9a is a very good approximation.

Accepting approximations I and IIa, and using them in eq II-3a, we find that the relationship between the q_j and $q_{j\pm1}$ is

$$(1-\delta)q_j(\infty) - (\gamma/2)(q_{j-1}^{(\infty)} + q_{j+1}^{(\infty)}) + \gamma\delta(1+\epsilon)q_j(\infty) - \beta C_a = 0 \qquad \text{(II-10a)}$$

On the other hand, eq II-5 gives

$$2\cosh\theta\, q_j(\infty) - (q_{j-1}^{(\infty)} + q_{j+1}^{(\infty)}) + 2q(1-\cosh\theta) = 0 \qquad \text{(II-10b)}$$

Equations II-10a and II-10b are consistent if

$$\gamma\cosh\theta = 1 - \delta + \gamma\delta(1+\epsilon) \qquad \text{(II-11)}$$

$$\gamma q(1-\cosh\theta) = -\beta C_a \qquad \text{(II-12)}$$

Observe that eq II-12 gives the correct form when $\beta = O(s(w^0)^{1/2} = 1)$, $q = 0$ and reproduces the $N = \infty$ limit exactly. Hence, we conclude that our approximate equilibrium solution for $q_j(\infty)$ is valid except for residues very close to the ends. This completes our discussion of the approximate equilibrium solution for the $q_j(\infty)$.

C. Approximate Time-Dependent Solution for $H(t)$. We are now in the position to construct an approximate master equation for $q_j(t)$, consistent with approximations I and IIa and valid in the moderate- to long-chain limit. Consider now the ratio $\langle \mu_j \mu_j^0 \mu_{j+1} \rangle / q_j$ in an infinite chain. This ratio for an infinite, homopolymeric, two-chain, coiled coil having $s = 0.94$ and $\sigma = 5 \times 10^{-4}$ slowly and monotonically increases from 0.9748 when $w^0 = 1.0$ to 0.9908 when $w^0 = 1.29$. For finite chain lengths, for example in a 284-residue, homopolymeric dimer, we find the above ratio $\langle \mu_j \mu_j^0 \mu_{j+1} \rangle / q_j$ with $j = 142$ equals 0.9775 and is accompanied by helix content 0.352 when $w^0 = 1.1317$ (where $s(w^0)^{1/2} = 1$) and the ratio equals 0.9758 and is accompanied by helix content 0.167 when $w^0 = 1.10$. Thus, we introduce *approximation IIb*: we assume eq II-9a is valid at all times, with ϵ characteristic of the final, equilibrium state. Approximation IIb should be valid provided the initial and final states are not too widely separated.

We now introduce *approximation III*. Since r_{jj^0}, r_{jj+1}, and $r_{j\pm1j^0}$ vary slowly as a function of w^0 provided the initial and final states are not too far apart, with the greatest variation occurring in r_{jj^0} and $r_{j\pm1j^0}$, and since the r_{jj^0}, $r_{jj\pm1}$, $r_{j\pm1j^0}$ relax twice as fast as the $q_j(t)$, we replace in eq II-3a

$$\frac{\beta\gamma}{2}(r_{j-1j} + r_{j+1j}) + \beta\delta r_{jj^0} - \frac{\beta\gamma\delta}{2}(r_{j-1j^0} + r_{j+1j^0})$$

by the values of the site–site correlations at infinite time, and use the approximate relation eq II-8a. This approximation in the master equation for $dq_j(t)/dt$ will be valid in two circumstances. The first circumstance occurs when the r_{jj^0}, $r_{j^0j\pm1}$, $r_{jj\pm1}$ of the initial and final states are fairly close together. For example, if $N = 284$, and w^0 equals 1.1317 and 1.10, respectively, the ratio of the r_{jj^0} with $j = 142$ in the initial to the final state is 0.9770. Similarly the ratio of the r_{j^0j-1} with $j = 142$ is 0.9765. Finally, the ratio of r_{jj-1} in the initial to final state with $j = 142$ is 0.9962. The second circumstance occurs when β is sufficiently small ($s(w^0)^{1/2}$ is near unity) so that the term proportional to β has a negligible effect on the time dependence of the $q_j(t)$.

Introducing approximations IIb and III into eq II-3a gives

$$dq_j/dt = -\alpha\{\gamma q_j \cosh\theta - (\gamma/2)(q_{j-1} + q_{j+1}) + \gamma q(1 - \cosh\theta)\} \quad \text{(II-13)}$$

which cosh θ defined in eq II-11.

However, since the $q_j(\infty)$ are related by eq II-10b, we have

$$d[q_j(t) - q_j(\infty)]/dt = -\alpha\{\gamma \cosh\theta[q_j(t) - q_j(\infty)] - (\gamma/2)[q_{j-1}^{(t)} - q_{j-1}^{(\infty)} + q_{j+1}^{(t)} - q_{j+1}^{(\infty)}]\} \quad \text{(II-14)}$$

Equation II-14b is a finite difference equation of the same form as 1-II-21; the solution to eq II-14b is

$$q_j^{(t)} = q_j^{(\infty)} + \frac{2}{N}\sum_{m=1}^{N-1}\sum_{k=1}^{N-1}[q_k(0) - q_k(\infty)] \sin\left(\frac{m\pi k}{N}\right) \sin\left(\frac{m\pi j}{N}\right) e^{-\alpha\nu_m t} \quad \text{(II-15a)}$$

wherein

$$\nu_m = \gamma[\cosh(\theta) - \cos(m\pi/N)] \quad \text{(II-15b)}$$

with $N - 1 \geq m \geq 1$.

Equations II-14a,b and II-15a,b reduce to the single-chain limit when $\beta = 0$ and $\delta = 0$, since cosh $\theta = 1/\gamma$, and are also consistent with the $N = \infty$ treatment introduced previously in paper 1 if ϵ is set equal to zero.

Moreover, it follows from eq II-15a that the mean overall helix content at time t, $\bar{q}(t)$, is

$$\bar{q}(t) = \bar{q}(\infty) + \frac{2}{(N)(N-1)}\sum_{\text{odd } m}^{N-1}\sum_{k=1}^{N-1}[q_k(0) - q_k(\infty)]\frac{\sin(m\pi k/N)\cos(m\pi/2N)e^{-\alpha\nu_m t}}{\sin(m\pi/2N)} \quad \text{(II-16)}$$

A quantity employed previously to characterize the relaxation rate is the initial slope of $H(t)$ defined in eq II-7.[11,17,18] In the context of our approximate treatment, the initial slope, which follows from eq II-14, is given by

$$-\left(\frac{dH}{dt}\right)_{t=0} = \alpha\left\{\gamma(\cosh\theta - 1) + \frac{\gamma}{(N-1)}\left[\frac{q_1(0) - q_1(\infty)}{\bar{q}(0) - \bar{q}(\infty)}\right]\right\} \quad \text{(II-17)}$$

with $q_1(t)$ the mean occupation number of residue one at time t. Observe that $\gamma(\cosh\theta - 1)$ is the rate associated with the slowest relaxing mode when $N = \infty$. The second set of terms, $[\gamma/(N-1)][(q_1(0) - q_1(\infty))/(\bar{q}(0) - \bar{q}(\infty))]$, corrects for the winding (or rewinding) of the ends and is always positive. Thus, eq II-17 implies that the initial slope probes the kinetics of the flipping of the same cooperative domains as in the infinite chain plus a contribution from the chain ends.

On the other hand, eq II-3a and II-3b provide us with the exact mean initial slope, wherein

$$\lambda_0 = \left(\sum_{j=1}^{N-1}\chi_j(0) - \chi_j(\infty)\right)/[(N-1)(\bar{q}(0) - \bar{q}(\infty))] \quad \text{(II-18)}$$

where $\chi_j(t)$ is defined in eq II-3b. The procedure for the calculation of the equilibrium values of the various correlation functions is found in the Appendix.

Up until this point, we have not specified how cosh θ is determined. If our approximate description of the dynamics is valid, we should be able to determine cosh θ from the exact initial slope defined in eq II-18 by

$$\cosh\theta = 1 + \frac{\lambda_0}{\gamma} - (N-1)^{-1}\left[\frac{q_1(0) - q_1(\infty)}{\bar{q}(0) - \bar{q}(\infty)}\right] \quad \text{(II-19)}$$

Substituting cosh θ determined from eq II-19 into eq II-6b should give the correct mean helix content, thus, providing a check on the validity of the approximations I–III. In eq II-19 as well as in eq II-15a and II-16, we employ equilibrium values for the q_j calculated from the exact equilibrium theory, viz., eq A-6. It should be pointed out that the above treatment is also applicable to isolated single chains if w^0 equals unity.

In this section, then, we have constructed an approximate analytical theory for the time dependence of the mean occupation number in a finite, two-chain, coiled coil that gives the correct initial slope and allows a calculation of the infinite-time, equilibrium value of the mean overall helix content, f_{hd}, that is consistent with approximations I–III. Thus, we shall regard the ability to correctly reproduce f_{hd} at infinite time as a measure of the validity of the approximate time-dependent solution derived in this section.

III. Numerical Results

A. Overview. In this section we shall examine the validity of our approximate formalism for the calculation of the time dependence of the mean helix content in two-chain, coiled coils. Then we shall examine the values of the initial slope λ_0 of the normalized time-dependent helix content, $H(t)$, vs. αt, defined in eq II-7, as well as the

Table I
Equilibrium Parameters of the Net Helix-to-Coil Transition in Two-Chain, Coiled Coils[a]

w^0_i	w^0_f	f_{hd}^i	f_{hd}^f (exact)	f_{hd}^f (approx)	R	$10^2\theta$
1.05	1.0	0.1018	0.08633	0.08598	0.9959	7.341
1.10	1.05	0.1673	0.1018	0.09831	0.9657	5.029
1.1317[b]	1.10	0.3520	0.1673	0.1594	0.9528	3.157
1.15	1.1317[b]	0.5405	0.3520	0.3626	1.030	2.526
1.17	1.15	0.7013	0.5405	0.5660	1.047	2.836
1.20	1.17	0.8180	0.7013	0.7247	1.033	3.805
1.25	1.20	0.8919	0.8180	0.8299	1.015	5.435
1.29	1.25	0.9185	0.8919	0.8872	0.9947	7.352

[a] All calculations were done on a homopolymeric, two-chain, coiled coil containing 284 residues per chain, with $\sigma = 5 \times 10^{-4}$ and $s = 0.94$. See text for definition of symbols. f_{hd}^f(approx) is calculated by employing eq II-6a–II-6c with θ obtained from eq II-19; i.e., the exact and approximate initial slopes of $H(t)$ are required to be equal. [b] This value of w^0 corresponds to helix–coil transition midpoint of an infinite dimer, that is $s(w^0)^{1/2} = 1.0$.

Table II
Equilibrium Parameters of the Net Coil-to-Helix Transition in Two-Chain, Coiled Coils[a]

w^0_i	w^0_f	f_{hd}^i	f_{hd}^f (exact)	f_{hd}^f (approx)	R	$10^2\theta$
1.0	1.05	0.08633	0.1018	0.1003	0.9852	5.756
1.05	1.10	0.1018	0.1673	0.1622	0.9695	3.364
1.10	1.1317[b]	0.1673	0.3520	0.3377	0.9593	2.136
1.1317[b]	1.15	0.3520	0.5405	0.5047	0.9338	2.124
1.15	1.17	0.5405	0.7013	0.6558	0.9351	2.675
1.17	1.20	0.7013	0.8180	0.7821	0.9561	3.916
1.20	1.25	0.8180	0.8919	0.8655	0.9704	5.969
1.25	1.29	0.8919	0.9185	0.9007	0.9806	7.888

[a] All calculations were done on a homopolymeric, two-chain, coiled coil containing 284 residues per chain, with $\sigma = 5 \times 10^{-4}$ and $s = 0.94$. See text for definition of symbols. f_{hd}^f(approx) is calculated by employing eq II-6a–II-6c with θ obtained from eq II-19; i.e., the exact and approximate initial slopes of $H(t)$ are required to be equal. [b] This value of w^0 corresponds to helix–coil transition midpoint of an infinite dimer, that is $s(w^0)^{1/2} = 1.0$.

validity of approximating $H(t)$ by $e^{-\lambda_0 \alpha t}$ as a function of different initial and final states. We then focus on the analogous properties in isolated, single-chain homopolypeptides, and a comparison of the time scale of the kinetics of helix → coil (or vice versa) transition in single chains and two-chain, coiled coils in the context of the kinetic Ising, neglect-loop-entropy, perfect matching model is made.

B. Application to Homopolymeric, Two-Chain, Coiled Coils. Unless otherwise indicated, all calculations on two-chain, coiled coils described below were performed on the approximate homopolymeric analogue of tropomyosin; i.e., each chain in the dimer contains 284 residues, each having the s (equal to 0.94) and σ (equal to 5×10^{-4}) chosen to approximate their respective geometric mean values in tropomyosin.[8]

In Tables I and II, we specify the initial-state and equilibrium, final-state values of the helix–helix interaction parameter (w^0_i and w^0_f, respectively), and the exact mean helix content in the dimer in the initial state and final state (f_{hd}^i and f_{hd}^f(exact), respectively), as given by the equilibrium theory (see eq 9 of ref 7). The value of f_{hd}^f(approx) is obtained from eq II-6b and II-6c; we also tabulate R, the ratio of f_{hd}^f(approx) to f_{hd}^f(exact). The value of θ is that required to give the exact initial slope employing eq II-19. If approximations I–III are valid, the entries in the fourth and fifth columns of Table I (and similarly in Table II) should be quite close.

In Table I, the equilibrium parameters of the net helix-to-coil transition are presented. Similarly in Table II, the equilibrium parameters of the net coil-to-helix transition are given. It is readily apparent from column 6 of Tables I and II that for the range of initial and final states chosen, the agreement of f_{hd}^f calculated via the approximate and exact methods is rather good (at worst R = 0.9528 and 0.9338 in Tables I and II, respectively, and in most cases lies even closer to unity).

For a given table the behavior of R may be rationalized as follows. If approximations I–III were exact, R would be identically unity. As w^0 increases (or decreases) to where the helix content of both the initial and final states lies in the plateau regime as a function of w^0, the initial and final values of the two-site and three-site correlation functions lie fairly close to each other. Approximations IIa and IIb and III therefore become better and R lies very near 1. In the region where the initial and final states differ more appreciably in helix content, the behavior is somewhat more complicated; while β is small and approximation III remains valid, approximation IIb, the replacement of ϵ by the value at the final state, is not as good, thereby giving rise to the larger values of R in the region where the helix content as a function of w^0 is the steepest.[8] However, since all the deviations in R from unity for the particular set of states chosen in Tables I and II are minor, it is apparent that approximations I–III are quite valid for these conditions. Hence, we have an approximate theory of the helix–coil or coil–helix transition that is capable of giving the exact initial slope, and, at the very worst, a final-state helix content within a few percent of the exact value.

Comparison of Table I, column 6, with Table II, column 6, for the same final state reveals the following. For $\beta < 0$ (i.e., $w^0 \leq 1.1317$) the initial and final states of the Table I are more widely separated, and thus R deviates further from unity in Table I than in Table II. For $\beta \geq 0$ (i.e., $w^0 \geq 1.1317$) the initial and final states are more widely separated in Table II than in Table I; thus, values of R lie closer to unity in the latter table than in the former table.

On the basis of Table I (Table II) we conclude that a temperature-jump (-drop) experiment employing a uniform temperature increment (decrement) probes the quasi-equilibrium regime at high and low temperatures, but probes the relatively large perturbation from equilibrium regime in the vicinity of the helix–coil (or vice versa) transition midpoint. A similar conclusion is found for infinite chains in paper 1.

Let us examine now the kinetics of a base line to base line experiment, i.e., one where initial and final states differ substantially. Consider the transition from an initial state $w^0_i = 1.29$ (helix content 0.9185) to a final state $w^0_f = 1.0$ (helix content 0.0863). The initial slope λ_0 for this transition is 1.235×10^{-3} and the f_{hd}^f(approx) = 0.0799. While the two-site correlation functions $r_{j,j}^0$, $r_{j^0,j\pm1}$, and $r_{j,j\pm1}$ differ between the initial and final states (e.g., in the infinite-chain limit, the values are 0.9467, 0.9466, and 0.9904 to be compared with 0.6569, 0.6569, and 0.9748, respectively), when $w^0 = 1$, $\delta = 0$; as is evident from eq II-3a we need only concern ourselves with $r_{j,j\pm1}$. Hence, approximation III remains satisfactory. In other words, we expect the approximate treatment to be valid for almost any practical temperature-jump experiment that can be performed. While the above is encouraging, it does not indicate that the approximations I–III are uniformly valid independent of initial and final states.

Let us now consider the results of the calculation where $w^0_i = 1.0$ and $w^0_f = 1.29$, and $\beta = 0.0327$, and $\delta \neq 0$. One now finds that the value of the cosh θ required to be consistent with the exact initial slope is less than unity,

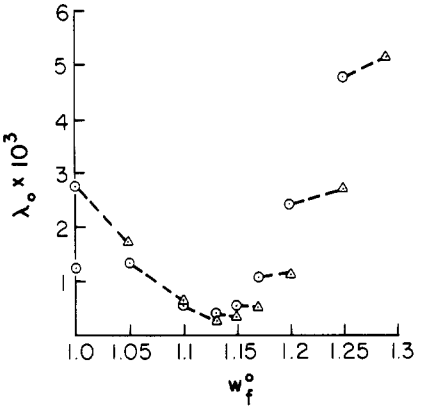

Figure 1. Plot of λ_0 calculated via eq II-18 vs. w^0_f, the helix–helix interaction parameter in a 284-residue, homopolymeric, two-chain, coiled coil having $\sigma = 5 \times 10^{-4}$ and $s = 0.94$. The net helix (coil) to coil (helix) transitions are denoted by circles (triangles). Pairs of initial and final states of the net coil-to-helix and net helix-to-coil transitions are connected by dotted lines; i.e., the w^0_i of a circle state corresponds to the w^0_f of a triangle state and vice versa.

an impossible and incorrect result. Thus, the approximations I–III, and in particular approximations IIb and III, are incorrect. We remind the reader that the various equilibrium quantities are very sensitive functions of β for small values of β. Thus, while the method is applicable to a wide range of initial and final states, caution must be exercised for the case of low helix going to high helix (analogous to a temperature-drop experiment).

In Figure 1 we have plotted λ_0 (calculated from eq II-18) vs. w^0_f (see also Table V). The net helix-to-coil transitions are denoted by circles and the net coil-to-helix transitions are denoted by triangles. For both kinds of transitions, net helix to net coil and vice versa, when $N = 285$, observe that there is a minimum in the curve of λ_0 vs. w^0_f where $s(w^0)^{1/2}$ equals unity, i.e., at $w^0_f = 1.1317$ (at the midpoint of the transition in the infinite chain). This is *not* however the midpoint of the transition of the 284-residue dimers whose helix content at $s(w^0)^{1/2} = 1.0$ is in fact only 35.2%. The minimum in λ_0 (or essentially equivalently in θ given in column 7, Tables I and II) reflects the fact that when $\beta = 0$ ($s(w^0)^{1/2} = 1$) coupling into the higher order, faster decaying site–site correlation functions is forbidden by the symmetry of the free energy of the system as shown in the discussion following eq 1-II-12b.[4] Setting $\beta \neq 0$ introduces additional bias toward the final state. $\beta > 0$ (<0) favors helix (random coil) states and, by allowing coupling into the faster modes, speeds up the transition. The presence of a minimum in λ_0 (maximum in the relaxation time) is in qualitative agreement with temperature-jump studies on the longer, two-chain, coiled-coil myosin rod.[19]

Let us now compare the high-to-low with the low-to-high helix-content transition between pairs of initial and final states denoted by dotted lines in Figure 1. If $\beta < 0$, i.e., where $s(w^0)^{1/2} < 1$, the state at lower helix content will have an $|\beta|$ that is larger and therefore a greater initial slope. Similarly, when β is appreciably greater than zero, the net coil-to-helix transition will have a larger β and thus will have a greater initial slope, as is clearly seen in Figure 1 for larger values of w^0_f. However, as w^0_f increases, the interchain cooperativity parameter δ also increases, and the larger the value of δ, the more cooperative the transition, and the slower the rate. For values of $\beta > 0$, but close to zero, the interchain cooperativity effect dominates (see section II, paper 1), and λ_0(helix → coil) > λ_0(coil → helix). As β increases, the biasing effect of the propagation parameter dominates and λ_0(coil → helix) > λ_0(helix → coil). Finally, the relative ordering at a given w^0_f of the λ_0 for the helix-to-coil and coil-to-helix transitions occurs for the identical reason as discussed above for the values of R in Tables I and II. It simply has to do with the fact that for $\beta > 0$ the helix → coil states are closer in helix content and for $\beta < 0$ the coil → helix states are closer in helix content. In all cases the cosh θ is an effective parameter reflecting the role played by the higher order correlation functions in the dynamics.

Insofar as the initial slope approximation to $H(t)$ is valid, i.e.

$$H(t) \sim e^{-\alpha\lambda_0 t} \tag{III-1}$$

we find that the time scale of the base line to base line experiments, $w^0_i = 1.0 \rightarrow w^0_f = 1.29$ with $\lambda_0 = 1.690 \times 10^{-4}$ and $w^0_i = 1.29 \rightarrow w^0_f = 1.0$ with $\lambda_0 = 1.235 \times 10^{-3}$ is quite close to the value where $\beta = 0$. That is, λ_0 equals 2.8687×10^{-4} for $w^0_i = 1.10 \rightarrow w^0_f = 1.1317$, and λ_0 equals 4.01×10^{-4} for $w^0_i = 1.15 \rightarrow w^0_f = 1.1317$. Hence, an important conclusion of the infinite-chain result remains correct for finite chains. Namely, measuring the transition rate to a final state where $s(w^0)^{1/2} = 1$ provides a reasonable estimate of the time scale in the experimentally more difficult (if not impossible), base line to base line experiments. (We point out that consistent with eq II-17 in the limit that $N \rightarrow \infty$, we recover an initial slope where $w^0_f = 1.1317$ ($\beta = 0$) independent of initial state and equal to 2.8632×10^{-4}). As would be expected, the initial slope for the infinite chain is less than coil → helix or helix → coil values of λ_0 for the $N = 284$ case presented above.

We now return to the question of the range of validity of approximating $H(t)$ by $e^{-\alpha\lambda_0 t}$. Given that eq II-17 is a valid approximation to the initial slope, it is apparent that if the ratio λ_0/ν_1 is very close to unity, with

$$\nu_1 = \gamma[\cosh\theta - \cos(\pi/N)] \tag{III-2}$$

then the distribution of frequencies is very narrow and the initial slope will be an excellent approximation for the characterization of the time dependence of $H(t)$. On the other hand, if the ratio λ_0/ν_1 differs substantially from unity, approximating $H(t)$ by $e^{-\alpha\lambda_0 t}$ will be inadequate. Basically then we require that

$$P = \left[\cosh\theta - \cos\left(\frac{\pi}{N}\right)\right]^{-1}\left[\cos\left(\frac{\pi}{N}\right) - 1 + \frac{(q_1(0) - q_1(\infty))}{(N-1)(\bar{q}(0) - \bar{q}(\infty))}\right] \ll 1 \tag{III-3}$$

It should be pointed out that approximation III implies that the initial slope and the slowest relaxing mode in the $N \rightarrow \infty$ limit are identical and are given by $\gamma(\cosh\theta - 1)$. The validity of this approximation with $\epsilon = 0$ has been demonstrated for the infinite-chain limit over a wide variety of initial and final states in section IV of paper 1. A similar conclusion for single-chain homopolypeptides has been found by Schwarz[17] and by Craig and Crothers.[18]

We show, in Figure 2A, $H(t)$ vs. αt for a 284-residue, homopolymeric dimer having $w^0_i = 1.10$ (initial-state helix content 0.1673) and $w^0_f = 1.1317$ (final-state helix content 0.3520). We find that $P = -0.006$. In other words the initial slope is *less* than the rate of the slowest relaxing mode, but the difference is negligible. This expectation is confirmed in Figure 2B, where we plot C_d, with

$$C_d = e^{\alpha\lambda_0 t}H(t) \tag{III-4}$$

vs. αt. The ratio is always close to but less than unity.

In Figure 3A we show $H(t)$ vs. αt for an initial state $w^0_i = 1.25$ (helix content 0.8919) and final state $w^0_f = 1.29$ (helix content 0.9185). For this set of conditions, $P = 0.62$.

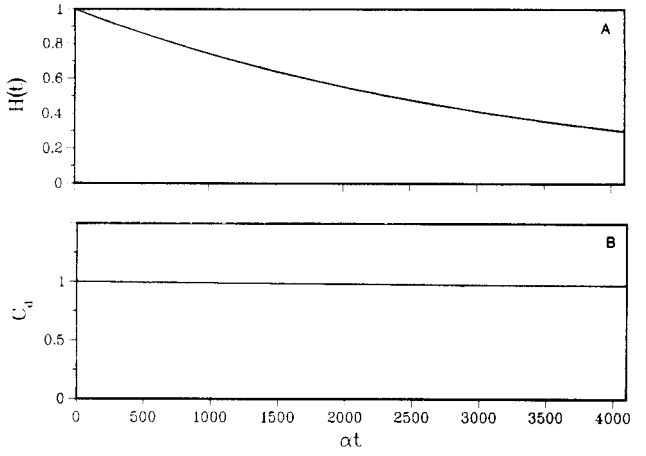

Figure 2. A: Plot of $H(t)$ vs. αt calculated via eq II-7 and II-16 for a 284-residue, homopolymeric, two-chain, coiled coil having $\sigma = 5 \times 10^{-4}$, and $s = 0.94$, with initial state $w^0_i = 1.10$ (helix content 0.1673) and final state $w^0_f = 1.1317$ (helix content 0.3520). B: Plot of C_d defined in eq III-4, vs. αt for the same conditions as in part A. The closer the values of C_d are to unity, the better is the initial slope approximation to $H(t)$.

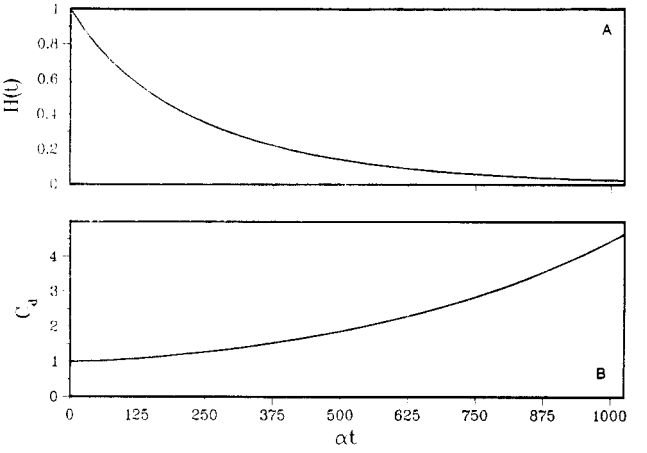

Figure 3. A: Plot of $H(t)$ vs. αt calculated via eq II-7 and II-16 for a 284-residue, homopolymeric dimer having $\sigma = 5 \times 10^{-4}$, and $s = 0.94$, with initial state $w^0_i = 1.25$ (helix content 0.8919) and final state $w^0_f = 1.29$ (helix content 0.9185). B: Plot of C_d defined in eq III-4 vs. αt for the same conditions as in part A. The closer the values of C_d are to unity the better is the initial slope approximation to $H(t)$.

The initial slope is 5.169×10^{-3}, not a very good approximation to the rate of smallest relaxing mode, ν_1, which is 3.170×10^{-3}. Otherwise stated, C_d vs. αt should rise above unity as αt increases. This is clearly seen in Figure 3B, where we display C_d vs. αt.

The above results are easily rationalized on the basis of eq II-16 and II-17. Basically the relaxation spectrum will be broad if the helix probability profile is quite curved, that is, where chain end effects are important. Otherwise stated, if the helix probability profile has a large number of Fourier components, then the relaxation spectrum in eq II-16 (and reflected in the second set of terms in eq II-17) will have appreciable contributions from all ν_m. Thus, the time dependence of $H(t)$ will be poorly characterized by the initial slope approximation. This occurs for chains where either N is relatively small or in the range where $q_1(0)$ and $q_1(\infty)$ differ substantially. It is in the limit of high helix content that the helix content of the ends is most sensitive to initial and final states and where $q_1(0)$ and $q_1(\infty)$ differ the most. Thus, as mentioned previously we conclude that $(N-1)^{-1}\gamma\{(q_1(0) - q_1(\infty))/(\bar{q}(0) - \bar{q}(\infty))\}$ is a measure of the effect of the curvature in the helix profile and at a given N will be most pronounced in the limit of higher helix content. In other words, the initial slope approximation to $H(t)$ breaks down for final states of high helix content, as is observed. The above considerations hold not only for dimers but also for single chains as discussed in section III-C.

By way of further illustration we have also done some representative calculations on a 284-residue-chain, homopolymeric, two-chain, coiled coil with $s = 0.94$ and the larger value of $\sigma = 10^{-2}$. With increasing σ, the helix–coil transition becomes less cooperative, and thus a 284-residue chain should be closer to the $N \to \infty$ limit. We have taken $w^0_i = 1.10$ (equilibrium helix content 0.4392) and $w^0_f = 1.1317$ (equilibrium helix content 0.4813). The initial slope approximation to $H(t)$ is excellent over the entire decay process and λ_0 is 1.468×10^{-2}. The approximate infinite-time helix content is 0.4811, in excellent agreement with the exact result. We then set $w^0_i = 1.25$ (helix content $f_{hd}^i = 0.6611$) and $w^0_f = 1.29$ (equilibrium helix content 0.7163). The initial slope approximation, while not as good as for the above case, nevertheless characterizes $H(t)$ to within 10% for values of $H(t) \geq 0.02$, clearly adequate for all practical purposes. The approximate equilibrium value of the helix content is 0.7180, again demonstrating the improved validity of the approximations I–III when the transition is less cooperative and the dimer effectively lies closer to the $N \to \infty$ limit.

As shown below, when $\sigma = 10^{-2}$ the approximate theory is capable of adequately handling the base line to base line kinetics from both high initial to low final helix content state and vice versa, unlike the case where $\sigma = 5 \times 10^{-4}$. For example, with $\sigma = 10^{-2}$, taking $w^0_i = 1.0$ ($f_{hd}^i = 0.3416$) and $w^0_f = 1.29$ (f_{hd}^f(exact) = 0.7163), we find an initial slope of 1.094×10^{-2}, which adequately characterizes $H(t)$ within 5% for $H(t) \geq 0.023$; initial and final states that are very far apart are generally well characterized by the slowest relaxing mode approximation for the initial slope; the ratio λ_0/ν_1 is 1.03. Moreover, f_{hd}^f(approx) equals 0.7117, clearly in adequate agreement with the exact value. Similarly, setting $w^0_i = 1.29$ and $w^0_f = 1.0$, we find an initial slope of $H(t)$ vs. αt of 1.951×10^{-2} and f_{hd}^f(approx) = 0.3408, in close agreement with the correct value. Note again that an estimate of the time scale of the base line to base line kinetics is readily obtained from examining the value of λ_0 when $\beta = 0$ and when the initial and final states are relatively close together.

C. Application to Single Chains. In order to obtain a comparison between the transition kinetics in two-chain, coiled coils and isolated single chains, we have performed a series of calculations on a homopolymeric single chain with $\sigma = 5 \times 10^{-4}$ as a function of different initial (final) state helix propagation parameters s_i (s_f) and exact equilibrium helix contents f_{hm}^i(f_{hm}^f(exact)). Comparison is made between f_{hm}^f(exact) and the approximate helix content consistent with the correct initial slope, f_{hm}^f(approx) (and obtained via eq II-6b, II-6c, and II-19).

The formalism derived in section II for two-chain, coiled coils is made applicable to single chains by setting $w^0 = 1$, so that $\delta = 0$, and β defined in eq II-4c equals $(s-1)/(s+1)$. We would in fact expect the approximate formalism introduced in section II to be an even better description of the dynamics in single chains. Approximations IIa and IIb are not needed, and at a given σ the helix–coil transition in isolated single chains is less cooperative than in dimers; in other words, at a given N, the single chain lies closer to the $N \to \infty$ limit.

In Tables III and IV, where we have presented the equilibrium parameters of the net helix-to-coil and net

Table III
Equilibrium Parameters of the Net Helix-to-Coil Transition in Single Chains[a]

s_i	s_f	f_{hd}^i	f_{hd}^f(exact)	f_{hd}^f(approx)	R	$10^2\theta$
0.97	0.94	0.1909	0.08633	0.08563	0.9919	7.066
1.00	0.97	0.4230	0.1909	0.1892	0.9910	5.118
1.03	1.00	0.6765	0.4230	0.4230	1.0000	4.473
1.06	1.03	0.8138	0.6765	0.6728	0.9945	5.174
1.09	1.06	0.8787	0.8138	0.8031	0.9869	6.529
1.12	1.09	0.9127	0.8787	0.8643	0.9836	8.028
1.15	1.12	0.9328	0.9127	0.8970	0.9827	9.510

[a] All calculations were done on a homopolymeric, isolated single chain containing 284 residues per chain with $\sigma = 5 \times 10^{-4}$. f_{hm}^f(approx) is calculated by employing eq II-6a–II-6c with θ obtained from eq II-19; i.e., the approximate and exact initial slopes of $H(t)$ are required to be equal.

Table IV
Equilibrium Parameters of the Net Coil-to-Helix Transition in Single Chains[a]

s_i	s_f	f_{hd}^i	f_{hd}^f(exact)	f_{hd}^f(approx)	R	$10^2\theta$
0.94	0.97	0.08633	0.1909	0.1932	1.012	5.894
0.97	1.0	0.1909	0.4230	0.4320	1.0000	4.473
1.0	1.03	0.4230	0.6765	0.6589	0.9740	4.572
1.03	1.06	0.6765	0.8138	0.7904	0.9712	5.773
1.06	1.09	0.8138	0.8787	0.8562	0.9744	7.311
1.09	1.12	0.8787	0.9127	0.8917	0.9770	8.856
1.12	1.15	0.9127	0.9328	0.9131	0.9789	10.33

[a] All calculations were done on a homopolymeric, isolated single chain containing 284 residues per chain with $\sigma = 5 \times 10^{-4}$. f_{hm}^f(approx) is calculated by employing eq II-6a–II-6c with θ obtained from eq II-19; i.e., the approximate and exact initial slopes of $H(t)$ are required to be equal.

coil-to-helix content transitions, respectively, the above conjectures are verified. In column 6 we show the ratio, R, of f_{hm}^f(approx)/f_{hm}^f(exact). The worst relative disagreement between the exact and approximate helix content is less than 2% for the net helix-to-coil transition and less than 3% for the net coil-to-helix transition. We remind the reader that the approximate theory becomes exact for single chains when s_f equals unity. It is apparent that the approximate treatment adequately handles the dynamics of single chains for the range of parameters employed. It will however break down if approximations I and III are incorrect, i.e., if the chains are very short and/or if the initial and final states are widely separated.

In Figure 4 we have plotted λ_0 calculated via eq II-18 vs. s_f with $\delta = 0$ and $\beta = (s - 1)/(s + 1)$. The transitions from net helix to coil (coil to helix) are denoted by circles (triangles). The slope of the λ_0 vs. s_f curve is seen to be steeper than the analogous curve displayed in Figure 1, for two-chain, coiled coils. As discussed in section IIIB, when $w^0{}_f$ increases, the interchain cooperativity parameter increases and this tends to decrease λ_0 (the more cooperative the transition, the larger is the domain size on the average that flips and the lower is the transition rate). On the other hand, there is a biasing parameter β that increases λ_0. The competition between these two effects produces the smaller slope in λ_0 vs. w_f in dimers as compared to λ_0 vs. s_f in single chains. In the case of isolated single chains there is no interchain cooperativity parameter, the increase in λ_0 from the minimum where $\beta = 0$ (no bias for helix or coil states) reflects only the increasing bias toward the final equilibrium state, and λ_0 increases more steeply, as is also observed in the infinite-single-chain case.[4] For the comparable range of initial and final states studied, the initial slopes in single chains are about a factor of 2–3 larger than in dimers. The relative ordering of λ_0 for the net helix-to-coil and coil-to-helix transitions follows the same β dependence as discussed above for dimers and will not be examined further.

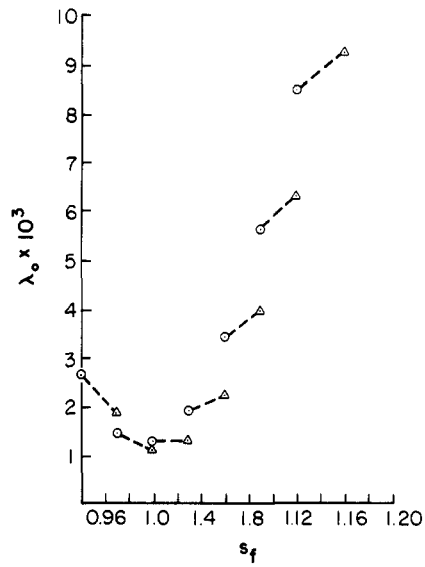

Figure 4. Plot of λ_0 vs. s_f for a 284-residue, homopolymeric, single chain with $\sigma = 5 \times 10^{-4}$. The net helix (coil) to coil (helix) transitions are denoted by circles (triangles). Pairs of initial and final states for the net coil-to-helix transition and net helix-to-coil transition are connected by dotted lines; i.e., the s_i of a circle state corresponds to the s_f of a triangle state and vice versa.

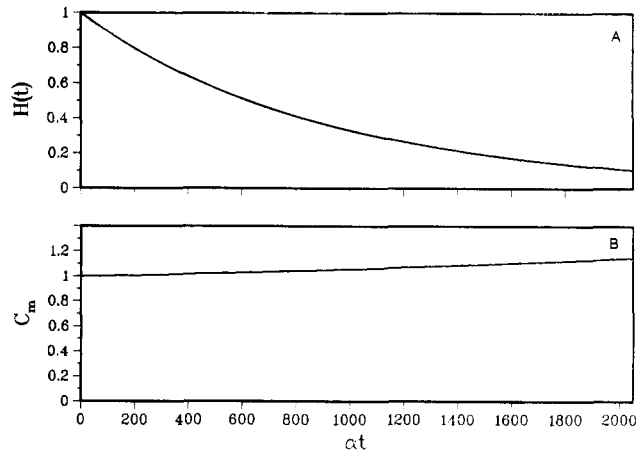

Figure 5. A: Plot of $H(t)$ vs. αt calculated via eq II-7 and II-16 for a 284-residue, single-chain homopolypeptide with $\sigma = 5 \times 10^{-4}$, $s_i = 0.97$ (helix content of 0.1909), and final state $s_f = 1.0$ (helix content of 0.4230). B: Plot of C_m defined in eq III-5 vs. αt for the same conditions as in part A. The closer the values of C_m are to unity, the better is the initial slope approximation to $H(t)$.

To further examine the validity of replacing $H(t)$ by $e^{-\alpha\lambda_0 t}$, we plot in Figure 5A $H(t)$ vs. αt for a single chain having an initial-state $s_i = 0.97$ (helix content 0.1909) and final-state $s_f = 1.0$ (helix content 0.4230), with initial slope 1.156×10^{-3} as compared to the $N \rightarrow \infty$ value of 9.99×10^{-4}. We remind the reader that the approximate theory is exact when $s_f = 1.0$. The ratio λ_0/ν_1 is 1.09. Thus, we would expect at longer times some deviations from the initial slope approximation, but nothing drastic. To verify this conjecture we plot in Figure 5B C_m given by

$$C_m = e^{\alpha\lambda_0 t}H(t) \qquad \text{(III-5)}$$

vs. αt. Since $C_m \leq 1.10$ for $H(t) \geq 0.18$, the process is fairly well characterized by the initial slope approximation, as would be expected by analogy to the discussion about the breadth of the relaxation spectrum in two-chain, coiled coils.

In Figure 6A, we plot $H(t)$ vs. αt for a single chain having an initial-state $s_i = 1.12$ (helix content 0.9127) and final-state $s_f = 1.15$ (helix content 0.9328), with $\lambda_0 = 9.288 \times 10^{-3}$. f_{hm}^f(approx) is 0.9131, in fairly good agreement with

Table V
Relaxation Parameters as a Function of Chain Length in Two-Chain, Coiled Coils[a]

		$N = 51$		$N = 101$		$N = 201$		$N = 285$	
w^0_i	w^0_f	$10^3\lambda_0$	λ_0/ν_1	$10^3\lambda_0$	λ_0/ν_1	$10^3\lambda_0$	γ_0/ν_1	$10^3\lambda_0$	λ_0/ν_1
1.05	1.0	5.588	0.9420	3.458	0.9721	2.883	1.002	2.775	1.007
1.10	1.05	3.893	0.9273	1.979	0.9462	1.426	0.9877	1.325	1.001
1.1317	1.10	2.669	0.9208	1.088	0.9270	0.6414	0.9745	0.5569	0.9968
1.15	1.1317	2.071	0.9287	0.7487	0.9480	0.4446	1.029	0.4007	1.056
1.17	1.15	1.814*	0.9538	0.6666*	1.030	0.5276	1.180	0.5494	1.188
1.20	1.15	1.626*	1.017	0.7258*	1.255	0.9427	1.433	1.069	1.363
1.25	1.20	1.506*	1.215	1.236*	1.848	2.152	1.762	2.414	1.571
1.29	1.25	1.297*	1.824	2.938*	2.536	4.239	2.013	4.761	1.724
1.0	1.05	4.088	0.9223	2.295	0.9585	1.825	1.003	1.737	1.012
1.05	1.10	2.637	0.8963	1.103	0.9074	0.6985	0.9751	0.6273	1.002
1.10	1.1317	1.979	0.8960	0.6601	0.8851	0.3394	0.9528	0.2869	0.9939
1.1317	1.15	1.708*	0.9148	0.5419*	0.9296	0.3248	1.040	0.3073	1.074
1.15	1.17	1.444*	0.9426	0.4720*	1.042	0.4456*	1.220	0.5053	1.208
1.17	1.20	1.119*	1.025	0.4929*	1.427	0.9165*	1.450	1.111	1.344
1.20	1.25	0.7714*	1.529	1.006*	2.290	2.314	1.673	2.719	1.477
1.25	1.29	0.7886*	3.895	2.927*	2.551	4.502	1.901	5.169	1.631

[a] All calculations were done on a homopolymeric, two-chain, coiled coil with $\sigma = 5 \times 10^{-4}$ and $s = 0.94$. λ_0 and ν_1 are calculated from eq II-18 and III-2, respectively. An asterisk indicates range of parameters for which the approximate analytic solution for $\bar{q}(t)$, eq II-16, has broken down.

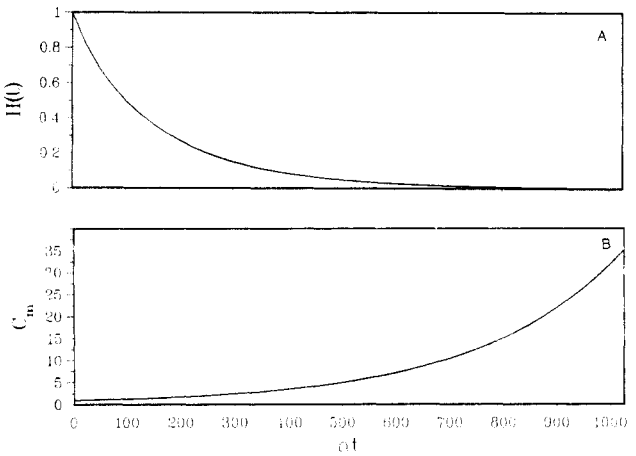

Figure 6. A: Plot of $H(t)$ vs. αt calculated via eq II-7 and II-16 for a 284-residue, single-chain homopolypeptide with $\sigma = 5 \times 10^{-4}$, $s_i = 1.12$ (helix content of 0.9127) and final state $s_f = 1.15$ (helix content 0.9328). B: Plot of C_m defined in eq III-5 vs. αt for the same conditions as in part A. The closer the values of C_m are to unity, the better is the initial slope approximation to $H(t)$.

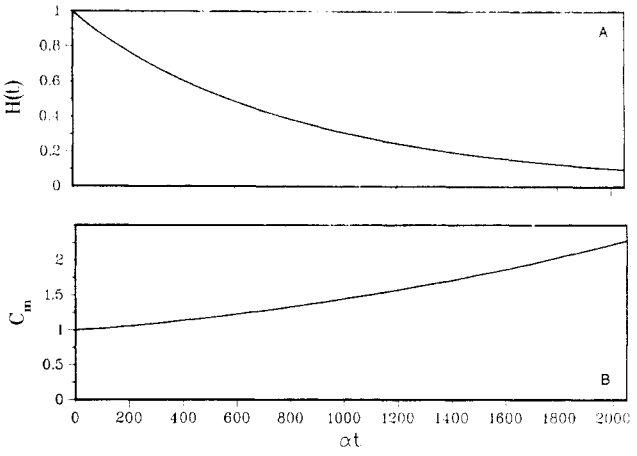

Figure 7. A: Plot of $H(t)$ vs. αt calculated via eq II-7 and II-16 for a 284-residue, single-chain, homopolypeptide with $\sigma = 5 \times 10^{-4}$, $s_i = 1.15$ (helix content of 0.9328), and $s_f = 0.94$ (helix content 0.086 33). B: Plot of C_m defined in eq III-5 vs. αt for the same conditions as in part A. The closer the values of C_m are to unity, the better is the initial slope approximation to $H(t)$.

the exact result. The slowest relaxing mode has ν_1 equal to 5.400×10^{-3}, giving a ratio λ_0/ν_1 of 1.72. This reflects the breadth of the spectral distribution. Clearly deviations in C_m from unity defined in eq III-5 are to be expected. In Figure 6B we have plotted C_m vs. αt; C_m is not well approximated by the initial slope, nor for the range of values of αt is it well approximated by $e^{-\alpha\nu_1 t}$. On the other hand, deviations form unity in C_m are not too large for times where $H(t)$ differs appreciably from zero. We point out that the deviations of C_m from unity are smaller than for the analogous set of initial and final states in dimers: Basically single chains have a narrower spectral distribution because for a given σ they are closer to the $N \to \infty$ limit, where the spectral distribution collapses to a single value (see eq II-17 as N goes to infinity).

In Figure 7A we have examined the base line to base line kinetics by a plot of $H(t)$ vs. αt, where $s_i = 1.15$ ($f_{hm}{}^i = 0.9328$) and $s_f = 0.94$ ($f_{hm}{}^f$(exact) = 0.08633). The initial slope of $H(t)$ vs. αt is 1.538×10^{-3} and $f_{hm}{}^f$(approx) = 0.08025. Observe that λ_0 is quite close to the value at $s_f = 1.0$ (and calculated assuming $s_i = 1.03$), namely 1.258×10^{-3}. The initial slope approximation to $H(t)$ is fair. ν_1 equals 1.072×10^{-3}; the ratio λ_0/ν_1 is 1.43. We plot in Figure 7B C_m vs. αt; some deviation in C_m from unity is evident over a majority of the relaxation process. This is merely a reflection that at long times the middle of the chain is still relaxing toward the equilibrium state whereas at short times the chain ends quickly reach their equilibrium state. Thus, a fairly broad relaxation spectrum is seen.

D. Effects of Chain Length. In Table V we study the initial slope and the ratio λ_0/ν_1 as a function of chain length for a homopolymeric two-chain, coiled coil with $\sigma = 5 \times 10^{-4}$ and $s = 0.94$. Chains of 50, 100, 200, and 284 residues are considered. As would be expected because of the increased curvature of the probability profiles at higher values of the helix content, approximations I–III break down for relatively short chains; and the time dependence of $\bar{q}(t)$ given in eq II-16 is not correct. Such cases are indicated by an asterisk in the entries of Table V. We again remind the reader tha the initial slope obtained via eq II-18 is exact for all N in the context of the kinetic Ising, neglect-loop-entropy model. We also point out that in the limit of large w^0, for a given w^0_i and w^0_f, the initial slope of a *shorter* chain is *smaller* than that of a *longer* chain. The origin of this effect is simple. The shorter chains are undergoing a transition from initial to final states whose

helix contents are more widely separated than those of the longer chains (a larger value of w^0 is required to obtain a given f_{hd}). Consider the case of initial-state $w^0_i = 1.29$ and final-state $w^0_f = 1.25$. When $N = 51$, $f_{hd}^i = 0.3164$, f_{hd}^f(exact) = 0.1928 and $\lambda_0 = 1.297 \times 10^{-3}$. However, if $N = 285$, $f_{hd}^i = 0.9185$, and $f_{hd}^f = 0.8912$, and $\lambda_0 = 4.761 \times 10^{-3}$. On the other hand, when the differences in helix content of initial and final states are similar, as for example when $w^0_i = 1.05$ and $w^0_f = 1.0$, then the smaller chains relax faster. If $N = 51$, $f_{hd}^i = 0.0530$, f_{hd}^f(exact) = 0.0499, and $\lambda_0 = 5.588 \times 10^{-3}$. If we set $N = 285$, $f_{hd}^i = 0.1018$, $f_{hd}^f = 0.0863$, and $\lambda_0 = 2.775 \times 10^{-3}$. Thus, one must be quite cautious on comparing relaxation data between chains of different length. Attention must be paid to both the initial- and final-state helix contents, i.e., whether the experiment involves a small or large perturbation from the initial-state helix content. It should be pointed out that the qualitative results discussed above for two-chain, coiled coils are also found for single chains; the single-chain results are not included here.

IV. Summary and Discussion of Results

In this paper we have extended the kinetic Ising, neglect-loop-entropy, perfect matching model of the helix–coil transition in two-chain, coiled coils to chains of moderate to infinite length. Starting from an approximate form of the equilibrium helix probability profiles, we have derived a time-dependent master equation consistent with the equilibrium, infinite-time limit. Analytic expressions are derived for the equilibrium occupation number of the jth residue, $q_j(\infty)$, and the mean overall occupation number $\bar{q}(\infty)$ as a function of a phase factor, θ, that relates the q_j to $q_{j\pm1}$. We then determine the phase factor by requiring that the exact initial slope λ_0 (readily determined from the exact master equation) and the initial slope determined in the approximate method agree (see eq II-19). Expressions for the time dependence of $q_j(t)$ and $\bar{q}(t)$ are given. We then calculate the helix content at infinite time from our approximate treatment. Provided that the initial and final states are not too far apart, excellent agreement between the exact and approximate equilibrium values of the helix content is found. Knowing $\cosh\theta$ allows us to obtain the rate of the slowest relaxing, long-wavelength mode, ν_1 (and in fact all modes). Comparison of the ratio λ_0/ν_1 allows us to measure the effective breadth of the spectral distribution *without having* to calculate the full relaxation curves. In other words, as discussed in section III-B (particularly eq III-2ff) we have a simple criterion for determining when the initial slope approximation to the normalized time-dependent helix content, $H(t)$, defined in eq II-7 is valid. In the limit of large chains, in agreement with Schwarz,[17] and Craig and Crothers,[18] we find a very narrow distribution of relaxation frequencies in single chains as well as in two-chain, coiled coils. On the basis of our analysis we conclude that the initial slope approximation to $H(t)$ at finite N where end effects are important breaks down when the initial and final states are widely separated or when the helix content is quite high.

These additional important qualitative conclusions emerge from our numerical analysis of the dynamics in two-chain, coiled coils and single chains at finite N:

(1) The initial slope of $H(t)$ vs. αt in both single chains and two-chain, coiled coils at finite chain length has a minimum when the final state has $s(w^0_f)^{1/2} = 1$ (where noninterfacial helical and randomly coiled states have equal statistical weights), i.e., at the transition midpoint (50% helix content) of an *infinite* chain. The minimum in λ_0 at finite N does not occur for the state that has 50% helix content.

(2) The increase in λ_0 vs. w_f to either side of $s(w^0_f)^{1/2} = 1$ reflects the role of the unequal statistical weights of random coil vs. helical states that produces a kinetic bias toward the final, equilibrium infinite-time state.

(3) The λ_0 vs. w^0_f curve in dimers is not as steep as the λ_0 vs. s_f curve in single chains because in the former case there is an additional interchain cooperativity parameter that increases as w_f increases. This tends to slow down the transition. Thus, at identical σ and N, the initial slope in single chains is about a factor of 2–3 larger than in two-chain, coiled coils for initial and final states having similar helix content. Furthermore, since the helix–coil transition in dimers is more cooperative than in single chains, at a given σ and N, the single chain lies closer to its infinite-chain limit than does a two-chain, coiled coil.

(4) At the level of approximation employed, the initial slope collapses to the slowest relaxing mode in the limit that $N \to \infty$. The slowest relaxing mode has Fourier components of wavelength N, i.e., the length of the chain (this merely corresponds to the fact that infinite-chain helix probability profiles are flat), and probes the dynamics of the cooperative domains of length on the order of $1/\sigma^{1/2}$ residues. The deviations of λ_0 from the slowest relaxing mode reflect the effects of curvature in the helix probability profile. The greater the curvature of the probability profile the larger the number of Fourier components. This gives rise to the greater contribution of the faster modes at finite N and higher values of the helix content to $H(t)$.

(5) Because of the shape of the curve of equilibrium helix content as a function of temperature,[13-15] temperature-jump (or -drop) experiments employing a uniform temperature increment (decrement) probe the quasi-equilibrium regime at high and low temperatures and the fairly large deviation from equilibrium regime in the vicinity of the transition midpoint. This conclusion depends only on the slope of the equilibrium helix content curve vs. temperature and is independent of the particular theory employed to describe the kinetics.

(6) The rate of decay in a base line to base line measurement (that is, a transition between a very high helix content initial state to a very low helix content final state, or vice versa) may be estimated by examining the kinetics of the helix–coil transition to a final state where the statistical weights of noninterfacial helical and random coil states are the same, i.e., $s(w^0_f)^{1/2} = 1$. Moreover, the initial slope for the final state having $s(w^0)^{1/2} = 1.0$ for a 284-residue chain is quite close to the value for an infinite two-chain, coiled coil and single chain when $\sigma = 5 \times 10^{-4}$.

(7) The initial slope approximation to $H(t)$ for a base line to base line experiment in the range of validity of our theory should be reasonably good for values of σ characteristic of tropomyosin, in both single chains and dimers.

It should be pointed out that for very short chains in the limit that σ goes to zero and s is less than unity, the only way to achieve a significant helix content in the present model of a two-chain, coiled coil is by having interacting helices, i.e., there is a single interacting helical stretch preceded and followed by randomly coiled tails in each of the chains. In this limiting case, the kinetic Ising, neglect-loop-entropy model reduces to the zipper model developed by Chay and Stevens,[20] and Miller,[21] and Jernigan, Ferretti, and Weiss.[22] However as σ and s are increased, in addition to an interacting helical stretch there will also be noninteracting helical stretches in each of the two chains, a situation that the zipper model is not designed to accommodate.

At this juncture, experimental measurements of the kinetics of the helix–coil transition in two-chain, coiled coils

are sorely needed. The various qualitative predictions described above need to be verified or disproved. Then guided by the results of experiments, the theory needs to be extended to include the roles of loop entropy, mismatch and mutual diffusion of the two chains in the dynamics; all of these present serious theoretical difficulties. However, it will be worth the effort if a cogent physical picture of the dynamics of the conformational transition in two-chain, coiled coils emerges.

Acknowledgment. This research was supported in part by a grant from the Biophysical Program of the National Science Foundation (No. PCM-8212404). Thanks are due to Professor Alfred Holtzer for his critical reading of the manuscript and many useful discussions and to Professor Robert Yaris for stimulating discussions.

Appendix. Equilibrium Correlation Functions of the Occupation Number: Finite Chains

In the calculation of the initial slope we needed equilibrium averages of various kinds of correlation functions of the occupation numbers; we present the prescription for their calculation in this Appendix. We refer the reader to Appendix B of ref 4 if the infinite-chain limits of these quantities are desired. We shall require the following statistical weight matrices:

$$A_{\mu_j} = \begin{bmatrix} -1 & \sigma s \\ -1 & s \end{bmatrix} \otimes \begin{bmatrix} 1 & \sigma s \\ 1 & s \end{bmatrix} E_w \qquad \text{(A-1)}$$

The statistical weight matrix for the mean occupation number of the jth residue in chain one, $\boldsymbol{E}_w$, is a diagonal matrix with unity everywhere on the diagonal except $E_w(4,4) = w^0$ and $\otimes$ denotes the direct product. Furthermore

$$A_{\mu_j{}^0} = \begin{bmatrix} 1 & \sigma s \\ 1 & s \end{bmatrix} \otimes \begin{bmatrix} -1 & \sigma s \\ -1 & s \end{bmatrix} E_w \qquad \text{(A-2)}$$

is the statistical weight matrix for the mean occupation number of the jth residue in chain two. Moreover

$$A_{\mu\mu^0} = \begin{bmatrix} -1 & \sigma s \\ -1 & s \end{bmatrix} \otimes \begin{bmatrix} -1 & \sigma s \\ -1 & s \end{bmatrix} E_w \qquad \text{(A-3)}$$

is the statistical weight matrix for calculation of the simultaneous occupation numbers of the jth residues in chains one and two. Finally, the statistical weight matrix associated with the jth residues in both chains

$$U_d = \begin{bmatrix} 1 & \sigma s \\ 1 & s \end{bmatrix} \otimes \begin{bmatrix} 1 & \sigma s \\ 1 & s \end{bmatrix} E_w \qquad \text{(A-4)}$$

The internal partition function of the dimer is

$$Z_{sd} = \mathbf{J}^* \prod_{i=1}^{N-1} \boldsymbol{U}_{di} \mathbf{J} \qquad \text{(A-5)}$$

$\mathbf{J}^*$ and $\mathbf{J}$ are Row(1,0,0,0) and Col(1,1,1,1) vectors, respectively.

The mean occupation number of the jth residue is

$$q_j = Z_{sd}{}^{-1} \mathbf{J}^* \prod_{i=1}^{j-1} \boldsymbol{U}_{di} \boldsymbol{A}_{\mu_j} \prod_{i=j+1}^{N-1} \boldsymbol{U}_{di} \mathbf{J} \qquad \text{(A-6)}$$

wherein we employ the convention $\prod_{i=n}^{m} \boldsymbol{U}_{di} = \boldsymbol{E}$, that is, the 4×4 identity matrix, if $n > m$.

We now consider two-site correlation functions of the occupation number.

If $j > 1$

$$r_{j,j-1} = Z_{sd}{}^{-1} \mathbf{J}^* \prod_{i=1}^{j-2} \boldsymbol{U}_{di} \boldsymbol{A}_{\mu_{j-1}} \boldsymbol{A}_{\mu_j} \prod_{i=j+1}^{N-1} \boldsymbol{U}_{di} \mathbf{J} \qquad \text{(A-7a)}$$

and if $j = 1$

$$r_{1,0} = -q_1 \qquad \text{(A-7b)}$$

the latter follows from the condition that phantom residue zero is always in the random coil state.

Similarly for all $N - 1 > j$

$$r_{j,j+1} = Z_{sd}{}^{-1} \mathbf{J}^* \prod_{i=1}^{j-1} \boldsymbol{U}_{di} \boldsymbol{A}_{\mu_j} \boldsymbol{A}_{\mu_{j+1}} \prod_{i=j+2}^{N-1} \boldsymbol{U}_{di} \mathbf{J} \qquad \text{(A-8a)}$$

and if $j = N - 1$

$$r_{N-1,N} = -q_{N-1} \qquad \text{(A-8b)}$$

since μ_N always equals minus one.

Now

$$r_{j,j^0} = Z_{sd}{}^{-1} \mathbf{J}^* \prod_{i=1}^{j-1} \boldsymbol{U}_{di} \boldsymbol{A}_{\mu\mu^0} \prod_{i=j+1}^{N-1} \boldsymbol{U}_{di} \mathbf{J} \qquad \text{(A-9)}$$

Moreover, if $j > 1$

$$r_{j^0,j-1} = Z_{sd}{}^{-1} \mathbf{J}^* \prod_{i=1}^{j-2} \boldsymbol{U}_{di} \boldsymbol{A}_{\mu_{j-1}} \boldsymbol{A}_{\mu_j{}^0} \prod_{i=j+1}^{N-1} \boldsymbol{U}_{di} \mathbf{J} \qquad \text{(A-10a)}$$

and if $j = 1$

$$r_{j^0,j-1} = -q_1 \qquad \text{(A-10b)}$$

If $j < N - 1$, we have

$$r_{j^0,j+1} = Z_{sd}{}^{-1} \mathbf{J}^* \prod_{i=1}^{j-1} \boldsymbol{U}_{di} \boldsymbol{A}_{\mu_j{}^0} \boldsymbol{A}_{\mu_{j+1}} \prod_{i=j+2}^{N-1} \boldsymbol{U}_{di} \mathbf{J} \qquad \text{(A-11a)}$$

and if $j = N - 1$

$$r_{j^0,j+1} = -q_{N-1} \qquad \text{(A-11b)}$$

We finally turn to the calculation of three-site correlation functions of the occupation number. If $j > 1$

$$\langle \mu_j \mu_j{}^0 \mu_{j-1} \rangle = Z_{sd}{}^{-1} \mathbf{J}^* \prod_{i=1}^{j-2} \boldsymbol{U}_{di} \boldsymbol{A}_{\mu_{j-1}} \boldsymbol{A}_{\mu\mu^0} \prod_{i=j+1}^{N-1} \boldsymbol{U}_{di} \mathbf{J} \qquad \text{(A-12a)}$$

and if $j = 1$

$$\langle \mu_1 \mu_1{}^0 \mu_0{}^0 \rangle = -r_{1,1^0} \qquad \text{(A-12b)}$$

Similarly, if $j < N - 1$

$$\langle \mu_j \mu_j{}^0 \mu_{j+1} \rangle = Z_{sd}{}^{-1} \mathbf{J}^* \prod_{i=1}^{j-1} \boldsymbol{U}_{di} \boldsymbol{A}_{\mu\mu^0} \boldsymbol{A}_{\mu_{j+1}} \prod_{i=j+2}^{N-1} \boldsymbol{U}_{di} \mathbf{J} \qquad \text{(A-13a)}$$

and if $j = N - 1$

$$\langle \mu_{N-1} \mu_{N-1}{}^0 \mu_N \rangle = -r_{N-1,N-1^0} \qquad \text{(A-13b)}$$

It should be pointed out that for homopolymers the values of q and $r_{j^0,j}$ are symmetric about the middle residue. In addition, the pairs $r_{j^0,j+1}$ and $r_{j^0,j-1}$, and $\langle \mu_j \mu_j{}^0 \mu_{j+1} \rangle$ and $\langle \mu_j \mu_j{}^0 \mu_{j-1} \rangle$ can be simply related to each other. Labeling the first member of each pair respectively by the indices $j,j+1$, and the second member of each pair by the indices $j,j-1$, we have by symmetry that the $j,j+1$ element of the first member equals the $N-j,N-j-1$ element of the second member. Hence, the amount of computer time required for the calculation of the various averages can be reduced by a factor of 2.

References and Notes

(1) Kim, P. S.; Baldwin, R. L. *Annu. Rev. Biochem.* **1982**, *51*, 459 and references cited therein.
(2) (a) Jaenicke, R., Ed. "Protein Folding, Proceedings of the 28th Conference of the German Biochemical Society"; Elsevier/

North Holland Biomed Press: Amsterdam, 1980. (b) Ghélis, C.; Yon, J. "Protein Folding"; Academic Press: New York, 1982.
(3) Lim, V. In ref 2a, p 149.
(4) Skolnick, J. *Macromolecules* **1984**, *17*, 2158.
(5) Glauber, R. J. *J. Math. Phys.* **1963**, *4*, 294.
(6) Zimm, B.; Bragg, J. K. *J. Chem. Phys.* **1959**, *31*, 526.
(7) Skolnick, J.; Holtzer, A. *Macromolecules* **1982**, *15*, 303.
(8) Skolnick, J. *Macromolecules* **1983**, *16*, 1069.
(9) Skolnick, J. *Macromolecules* **1983**, *16*, 1763.
(10) Skolnick, J. *Macromolecules* **1984**, *17*, 2153.
(11) Schwarz, G. *Biopolymers* **1968**, *6*, 873.
(12) Ishiwari, K.; Nakajima, A. *Macromolecules* **1978**, *11*, 785.
(13) Lehrer, S. *J. Mol. Biol.* **1978**, *118*, 209.
(14) Holtzer, M. E.; Holtzer, A.; Skolnick, J. *Macromolecules* **1983**, *16*, 173.
(15) Hodges, R.; Saund, A.; Chong, P.; St. Pierre, S.; Reid, R. *J. Biol. Chem.* **1981**, *256*, 1214.
(16) Tanaka, T.; Wada, A.; Suzuki, M. *J. Chem. Phys.* **1973**, *59*, 3799.
(17) Schwarz, G. *J. Mol. Biol.* **1965**, *11*, 64.
(18) Craig, M. E.; Crothers, D. *Biopolymers* **1968**, *6*, 385.
(19) Tsong, T. Y.; Himmelfarb, S.; Harrington, W. F. *J. Mol. Biol.* **1983**, *164*, 431.
(20) Chay, T. R.; Stevens, C. L. *Biopolymers* **1973**, *12*, 2563.
(21) Miller, W. G. *Macromolecules* **1973**, *6*, 100.
(22) Jernigan, R. L.; Ferretti, J. A.; Weiss, G. H. *Macromolecules* **1973**, *6*, 684.

Liquid–Liquid Phase Separation in Multicomponent Polymer Systems. 22. Thermodynamics of Statistical Copolymers†

Ronald Koningsveld* and Ludo A. Kleintjens

DSM, Research and Patents, 6160 MD Geleen, The Netherlands. *Received March 10, 1984*

ABSTRACT: Limits of thermodynamic stability (spinodals) and critical points in liquid systems containing statistical copolymers are investigated numerically on the basis of the classic lattice model. The calculated phase behavior reproduces the scarce experimental data in the literature in a qualitatively correct manner, provided the model is extended to allow for the various constitutional repeat units (CRUs) to differ in number of nearest-neighbor contacts. In particular, the sensitivity of phase relations toward small changes in chemical composition and/or chain length is reproduced. Multiplicity of critical points may be expected to arise easily and, with it, separations into three phases. The latter is in accordance with observations reported several years ago by Molau. Whether or not a third copolymer compatibilizes a mixture of two (co)polymers seems to depend subtly on the molecular characteristics mentioned and on the pair interactions between the various CRUs.

Compared with homopolymers statistical copolymers have so far not received the attention in the thermodynamic literature one would expect on account of their practical importance. Their complex molecular structure may explain this apparent negligence, studies of homopolymers already being up against formidable difficulties.

In this paper we focus on liquid–liquid phase relationships in mixtures containing statistical copolymers. We exclude dilute-solution properties from the discussion which thus covers systems in which the segment density can to a good approximation be considered uniform. The molecular model used is based on the rigid lattice treatment of Flory, Huggins, and others, amended to deal with the situation in hand.[1-6]

Among the systems of interest we have solutions of copolymers in a single solvent where the influences of chemical composition and chain length could be explored theoretically. Another system of practical importance is a partially miscible blend of two chemically different homopolymers in which a statistical copolymer might have a compatibilizing effect. The copolymer may or may not consist of the monomers in the two homopolymers. The first case has recently been studied theoretically by Leibler.[7] The investigation of the systems mentioned is complicated by the fact that two statistical copolymers, having the same chain length but differing in monomer content, are not necessarily miscible in all proportions. This conclusion came out of a theoretical analysis by Scott,[6] and it was subsequently experimentally verified by Molau[8] and by Locatelli and Riess,[9] for copolymers of styrene and acrylonitrile (SAN). With the molar masses Molau used, a difference in AN content of only 4 mol % already sufficed to bring about partial miscibility. This effect, caused by the decrease the entropy of mixing per unit volume undergoes upon stringing the two types of repeat units together, is also present if the copolymers are dissolved in a common solvent. The tolerable difference in chemical composition is then (understandably) found to become larger when the dilution is increased.

A similar investigation of solvent-free copolymer mixtures was carried out by Kollinsky and Markert,[10,11] who used various acrylic monomers. The tolerable composition difference proved to depend on the chemical structure and this finding could later be analyzed thermodynamically on the basis of Scott's treatment, if properly amended for the relative sizes of the monomer units.[12]

Whereas solvent-free systems only call for a single parameter for the interaction between the two types of repeat units, addition of a solvent (which leads to at least a binary solution) brings two additional parameters, one for each of the solvent–segment interactions. It has been tried to circumvent the complication by the introduction of a single "effective" interaction parameter which represents a linear interpolation between the two solvent–homopolymer parameters, i.e.

$$g = g_{o\alpha}\phi_\alpha + g_{o\beta}\phi_\beta \tag{1}$$

where g is the effective interaction parameter, $g_{o\alpha}$ and $g_{o\beta}$ are the solvent–homopolymer interaction parameters (α and β refer to the two types of repeat units), and ϕ_α (=1 − ϕ_β) is the α content of the copolymer. This approach has been followed inter alia by Lautout-Magat,[13,14] Topchiev et al.,[15] and Teramachi et al.[16,17]

† Presented in part at the 24th Microsymposium "Copolymers: Structure and Solution Properties", Prague, July 1983.

0024-9297/85/2218-0243$01.50/0